

Breakup of H_2 in Singly Ionizing Collisions with Fast Protons: Channel-Selective Low-Energy Electron Spectra

C. Dimopoulou,¹ R. Moshhammer,¹ D. Fischer,¹ C. Höhr,¹ A. Dorn,¹ P. D. Fainstein,⁴ J. R. Crespo López Urrutia,¹
C. D. Schröter,¹ H. Kollmus,² R. Mann,² S. Hagmann,^{2,3} and J. Ullrich¹

¹Max-Planck-Institut für Kernphysik, Saupfercheckweg 1, 69117 Heidelberg, Germany

²Gesellschaft für Schwerionenforschung, Planckstrasse 1, 64291 Darmstadt, Germany

³Institut für Kernphysik, August-Euler-Strasse 6, 60486 Frankfurt, Germany

⁴Centro Atómico Bariloche, Comisión Nacional de Energía Atómica, 8400 Bariloche, Argentina

(Received 25 March 2004; published 17 September 2004)

Dissociative as well as nondissociative single ionization of H_2 by 6 MeV proton impact has been studied in a kinematically complete experiment by measuring the momentum vectors of the electron and the H^+ fragment or the H_2^+ target ion, respectively. For the two ionization pathways, the electron spectra reveal the role of autoionization of the doubly and singly excited states of H_2 . The latter explicitly involve the coupling between the electronic and the nuclear motion of the molecule. This is a clear manifestation of a breakdown of the Born-Oppenheimer approximation.

DOI: 10.1103/PhysRevLett.93.123203

PACS numbers: 34.50.Gb, 33.80.Eh

Single ionization of atoms by fast ion impact has been studied extensively for many years [1,2]. Fully differential cross sections (FDCS), as available for electron impact ionization since 1969 (for a review see [3]), have not become experimentally accessible before 2000 with many surprising results (for a review see [4]). As far as molecular targets are concerned, H_2 has been the prototype system because it is the simplest diatomic molecule (see e.g. [1,5,6]) and has attracted considerable recent attention [7]. The molecular nature of the target introduces new aspects to the collision problem due to the shape of the target potential, the coupling between electronic and nuclear motion giving rise to additional channels, and the two-center geometry of the target leading to interference effects in analogy to Young's two-slit experiment [8]. Moreover, charged particle induced ionization of molecules plays a central role in many applications like, e.g., cancer therapy with fast ions. There, the production of low-energy electrons is of particular relevance because they effectively destroy large molecules in biological tissue [9].

Two possible pathways can be distinguished in single ionization of H_2 (Fig. 1). First, in what we call pure ionization, a stable, possibly vibrationally excited H_2^+ ion remains after the removal of the electron. Second, with a small probability of a few percent of all ionization events [6,10], the molecule dissociates into an H^+ and an H atom (dissociative ionization). The latter happens either by the creation of an excited molecular ion which dissociates since all $(H_2^+)^*$ states are repulsive in the Franck-Condon region or by populating the vibrational continuum of the ground state of H_2^+ , resulting into dissociation into an H^+ and an H(1s) (ground state dissociation). Most detailed information about the contribution of all channels and the dynamics involved can be obtained in

an electron-ion coincidence experiment. For instance, ionization plus excitation (channel 2a in Fig. 1) can be separated from ground state dissociation (channel 2b) using the fact that the kinetic energy of the H^+ from the former is typically of the order of a few eV, whereas from the latter it is in the sub-eV range [11]. Until now the experiments have detected either the emitted electron [5,7,10] or the nuclear fragments (see [6] and references

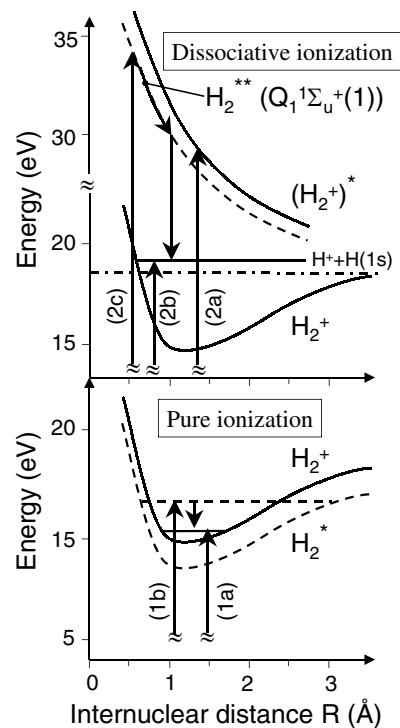


FIG. 1. Schematic potential curves for H_2 and H_2^+ illustrating the different single ionization pathways (for detailed potential curves see [24,25]).

therein). Only one coincident measurement has been performed [12], but at much lower collision energies.

In this Letter we report on the coincident detection of the electron and the charged nuclear fragments resulting from single ionization of H_2 by proton impact (projectile velocity: $v_p = 15.5$ a.u.). Using a “reaction microscope” [4] we have recorded the electron energy spectra resolved down to 0.1 eV for both dissociative and pure ionization. For the latter the measurement represents a kinematically complete experiment, whereas this is not the case for the former since the H atom has not been detected. Within the same frame, FDCS have been obtained for pure ionization, which, to our knowledge, have not been accessible so far for ion impact on H_2 . It has been frequently argued (see [7] and references therein) that, as far as single ionization is concerned, the cross section of H_2 is equal to that of 2 H atoms times an oscillatory term representing the interference caused by the coherent electron emission from the two centers. The comparison of our data with predictions of a continuum-distorted-wave eikonal-initial-state (CDW-EIS) calculation [13] taking such interference effects into account provides convincing evidence that this is not true, at least not for low-energy electron emission. Distinct differences appear that can be explained only by taking into account the molecular nature of the target. Here, particular attention will be given to the autoionization of singly and doubly excited states of H_2 , effects that involve not only the electronic but also the nuclear motion of the molecule.

The experiment was performed at the Max-Planck-Institute in Heidelberg using a multielectron recoil ion momentum spectrometer (reaction microscope [4]). A well-collimated (1 mm \times 1 mm), pulsed (pulse length \approx 1 ns, repetition rate = 289 kHz) proton beam (beam current = 0.5 nA) with an energy of 6 MeV crosses a beam of H_2 provided by a gas jet. The target molecules are in the vibrational ground state, since they reach a temperature of less than 10 K after the supersonic expansion. The emitted electrons and the recoil ion were extracted into opposite directions along the projectile beam axis (longitudinal direction) by a weak (4.5 V/cm) electric field over 11 cm and were detected by two-dimensional position sensitive detectors. A uniform longitudinal magnetic field of 14 G confined the transverse motion of the electrons, such that all electrons with energy $E_e < 35$ eV were detected with the full solid angle. The momentum vectors of both, recoil ion (H_2^+ or H^+) and electron, are determined from their measured absolute times of flight and positions on the detectors. The H_2^+ ions were detected for transverse momenta $p_{\perp} \leq 2.9$ a.u., covering essentially the full solid angle for pure ionization. For the H^+ ion, the acceptance was $p_{\perp} \leq 2.3$ a.u., corresponding to energies of less than 40 meV for $p_{\parallel} = 0$, covering a solid angle of approximately 10% for ground state dissociation. The achieved momentum

resolution for the H_2^+ recoil ions was $\Delta p_{r\parallel} = 0.1$ a.u. in the longitudinal and $\Delta p_{r\perp} = 0.3$ a.u. in the transverse direction. For the electrons we estimated $\Delta p_{e\parallel} \approx 0.05$ a.u. and $\Delta p_{e\perp} = 0.1$ a.u., respectively. The transverse momentum transfer is calculated event by event from the transverse momenta of the electron and the H_2^+ ion $\mathbf{q}_{\perp} = (\mathbf{p}_{e\perp} + \mathbf{p}_{r\perp})$ with an estimated resolution of $\Delta q_{\perp} \approx 0.3$ a.u. The total momentum transfer is given by $\mathbf{q} = \mathbf{q}_{\perp} + q_{\min} \cdot \hat{U}_p$, where \hat{U}_p is the unit vector along the initial projectile velocity. The small quantity $q_{\min} = (I + E_e)/v_p < 0.1$ a.u. is the minimum momentum transfer required to overcome the binding energy $I = 15.4$ eV and eject an electron with energy E_e .

The electron energy distributions for pure and dissociative ionization as well as the theoretical cross sections calculated within the CDW-EIS are shown in Fig. 2(a). In the theoretical model the initial state of H_2 is approximated by a superposition of two hydrogenic orbitals centered at each nucleus with a separation given by the equilibrium internuclear distance ($R = 1.4$ a.u.) and an effective charge of $Z_{\text{eff}} = 1.19$ to correctly reproduce the electronic binding energy. The resulting cross section for emission of an electron with momentum vector \mathbf{k}_e is equal to the one for ionization of two “effective” H atoms multiplied by $(1 + \sin\chi/\chi)$, $\chi \equiv |\mathbf{k}_e - \mathbf{q}|R$, which represents the interference caused by the two centers for random orientation of the molecular axis (for details see [13]). The CDW-EIS calculation predicts a total cross

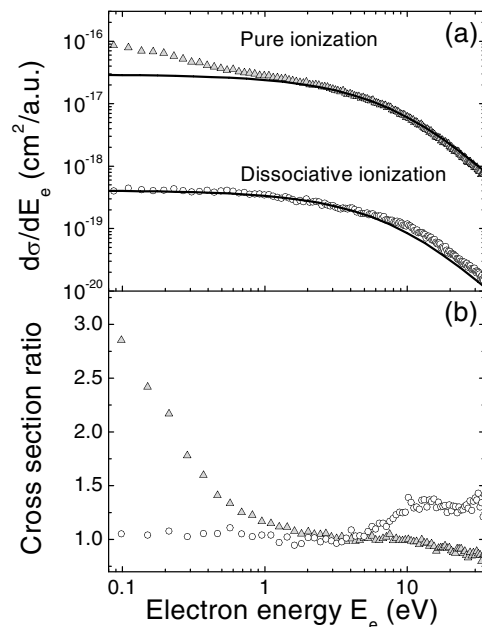


FIG. 2. (a) Electron energy distributions for single ionization of H_2 by 6 MeV proton impact. Triangles: experimental results for pure ionization; circles: experimental results for dissociative ionization (for H^+ energies smaller than 40 meV); solid lines: CDW-EIS results. (b) Ratios of experimental to theoretical cross sections.

section for $E_e \leq 35$ eV of $\sigma_{\text{H}_2^+} = 7.35 \times 10^{-18}$ cm². The experimental cross section $d\sigma_{\text{H}_2^+}/dE_e$ for pure ionization has been normalized to the theoretical one in the region $2 \text{ eV} \leq E_e \leq 35 \text{ eV}$. The experimental cross section $d\sigma_{\text{H}^+}/dE_e$ has been normalized to the known contribution of ground state dissociation, which is 1.4% of $\sigma_{\text{H}_2^+}$ [6,10], assuming the electron emission to be independent on the energy and angular distribution of the H₂, as follows from our data.

Two main features appear in the electron spectra. First, the data from pure ionization are in reasonable agreement with the CDW-EIS calculation except for $E_e < 1$ eV where a significant enhancement of the cross section is observed. This feature is absent for dissociative ionization indicating that it is not a signature of the molecular wave functions, which are clearly not properly described in the CDW-EIS. Second, at E_e around 12 eV a distinct difference appears in the shape of the cross sections between pure and dissociative ionization. These structures become more visible in the ratios between the data and the CDW-EIS calculation for both pathways [Fig. 2(b)]. In what follows, these two features will be discussed separately.

The enhancement of the cross section for pure ionization in the sub-eV region is due to the presence of autoionizing channels, which lead to the ejection of very low-energy electrons by a uniquely molecular mechanism. From high-resolution studies [14,15] and systematic theoretical work [16,17], it is well established that photo-

ionization of H₂ just below and within the first eV above threshold (more precisely from 15.3 to 16.6 eV) is dominated by autoionization from rovibrational levels of singly excited bound Rydberg states of H₂. As depicted in Fig. 1 (channel 1b), their potential curves lie within a few eV below the ground state of H₂⁺ and are essentially parallel to it, particularly for those with a quantum number of the Rydberg electron $n \geq 4$. Higher vibrational levels of these states have energies above the ionization potential of H₂ and therefore autoionize by converting energy from the vibrational motion into kinetic energy of the outgoing electron: The electron can be viewed to autoionize by scattering on the ion core. This process is known as vibrational autoionization [18] and is an explicit example of the breakdown of the Born-Oppenheimer approximation.

Differences between this vibrational autoionization (channel 1b) and the direct ionization to the continuum (channel 1a) are expected to become evident in FDCS. In Fig. 3 (upper row) we present the FDCS $d^5\sigma/d\mathbf{q}_\perp d\mathbf{k}_e$ for electrons emitted into the scattering plane, i.e., the plane defined by the momentum vectors of the incoming and the scattered projectile, as a function of the polar electron emission angle relative to the initial projectile direction, for a fixed $E_e = 2.6$ eV and two different values of the momentum transfer q . As expected for the direct ionization (channel 1a) the agreement between the data and the CDW-EIS on an absolute scale is reasonably good. The large peak (the so-called binary peak [3]) in the direction

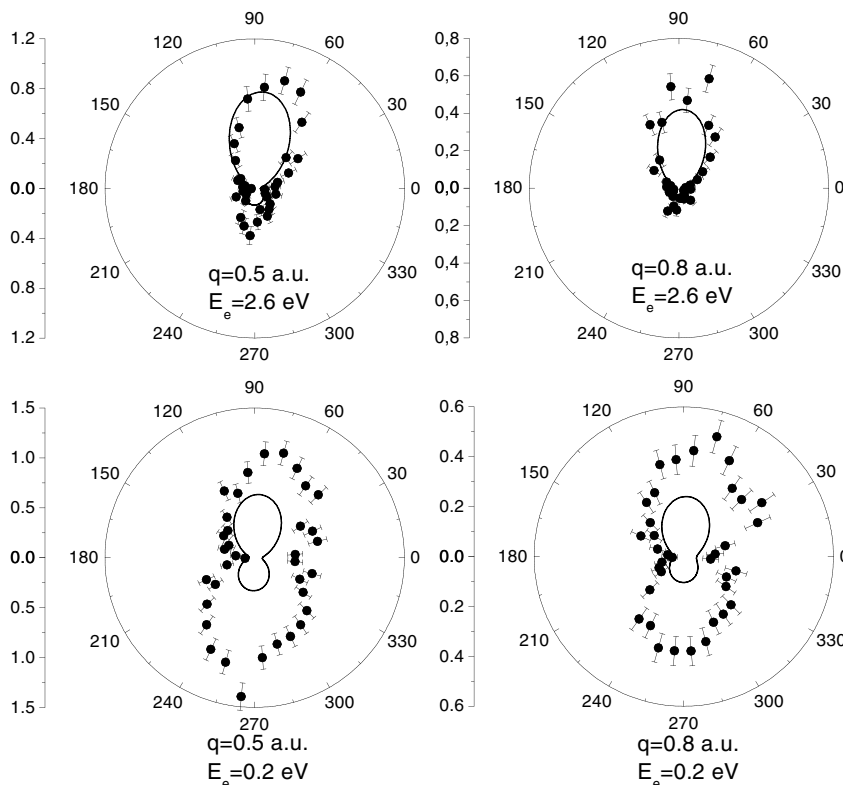


FIG. 3. FDCS for electrons emitted into the scattering plane for pure ionization of H₂ by 6 MeV proton impact. Upper row: The electron energy $E_e = 2.6$ eV is fixed and the values of the momentum transfer are $q = 0.5, 0.8$ a.u.. Lower row: $E_e = 0.2$ eV, same values of q . Solid lines: CDW-EIS results. The cross sections are given in 10^{-18} cm²/a.u.².

of \mathbf{q} (practically at 90°) corresponds to electrons ejected by a binary interaction with the projectile, whereas the smaller peak in the direction of $-\mathbf{q}$ (the so-called recoil peak) corresponds to the case when most of the momentum transfer is taken by the recoil ion. As q increases the recoil peak systematically decreases in magnitude relative to the binary peak.

At $E_e = 0.2$ eV the comparison of the FDCS with the CDW-EIS reveals distinct discrepancies (lower row in Fig. 3), not only in the magnitude of the cross sections, as expected from Fig. 2, but more severely, in the absolute value and the q dependence of the ratio between the recoil and the binary peak. This ratio is close to 1 and does not change with increasing q , a feature that can be understood for vibrational autoionization (channel 1b): Making use of the analogy between charged particle impact excitation (ionization) and photoionization for small q and E_e [19], we expect that the angular distribution of the autoionized electrons is essentially a dipolar one with respect to the momentum transfer axis. In fact, the autoionization can be described as a dipolelike photoexcitation of the H_2 to a bound intermediate electronic state followed by a transition of the electron into a continuum p state after transfer of energy from the vibrating nuclei to the electron, leaving the H_2^+ ion in its $1s\sigma_g$ ground state.

Returning to the dissociative ionization, a broad maximum appears in comparison with the CDW-EIS prediction at E_e around 12 eV up to 35 eV, as shown in Fig. 2(b). This feature can be explained by the contribution of an additional channel, namely, the excitation of a doubly excited state of H_2 autoionizing by an electronic transition into the vibrational continuum of the ground state of H_2^+ , as depicted by channel 2c in Fig. 1. After excitation to the H_2^{**} state the atoms gain kinetic energy ΔE as they separate along the repulsive curve. At some internuclear distance the molecule autoionizes and, if ΔE is sufficiently large, it dissociates into an H^+ and an $\text{H}(1s)$. Ion [20], electron [10], and photon [21,22] impact studies have shown the importance of H_2^{**} states in dissociative ionization of H_2 . In [10,21,22] the ratio of the yield of H^+ with respect to H_2^+ ions has been measured as a function of the energy transferred to the molecule. Although the first excited state ($2p\sigma_u$) of H_2^+ is not accessible in the Franck-Condon region at energies below 28 eV, a broad maximum appears at around 30 eV. For very low-energy H^+ , as it is the case in our experiment, an additional small structure appears close to 25 eV. Calculations [23] have attributed the maximum at 30 eV to channel 2c and the structure at 25 eV to its interference with channel 2b (Fig. 1). Given that 18.1 eV is the threshold for ground state dissociation, the above structures correspond to the observed enhancement at E_e around 12 eV.

In summary, the electron energy spectra for pure ionization of H_2 and that coincident with dissociation have

been measured. Surprisingly, significant differences are observed between pure and dissociative ionization although the kinetic energy released in the dissociation amounts to only a few tens of meV. The comparison with the CDW-EIS predictions allowed the identification of sizeable contributions from molecule-specific channels. The observed differences are due to the autoionization of singly or doubly excited states of H_2 , which decay through the coupling between the nuclear and the electronic motion in the molecule. In this respect, the experiment sets a challenge to the atomic collision theory extended to molecular targets.

We acknowledge support from the EU within the HITRAP Project (HPRI-CT-2001-50036) and from the DAAD-Fundación Antorchas cooperation program. We are grateful to A. Voitkiv and B. Najjari for numerous discussions.

-
- [1] M. E. Rudd *et al.*, Rev. Mod. Phys. **64**, 441 (1992).
 - [2] N. Stolterfoht, R. D. DuBois, and R. D. Rivarola, *Electron Emission in Heavy Ion-Atom Collisions*, Springer Series on Atoms and Plasmas (Springer, New York, 1997).
 - [3] A. Lahmam-Bennani, J. Phys. B **24**, 2401 (1991).
 - [4] J. Ullrich *et al.*, Rep. Prog. Phys. **66**, 1463 (2003).
 - [5] L. H. Toburen and W. E. Wilson, Phys. Rev. A **5**, 247 (1972).
 - [6] I. Ben-Izthak *et al.*, J. Phys. B **29**, L21 (1996).
 - [7] N. Stolterfoht *et al.*, Phys. Rev. Lett. **87**, 023201 (2001).
 - [8] H. D. Cohen and U. Fano, Phys. Rev. **150**, 30 (1966).
 - [9] B. Boudaiffa *et al.*, Science **287**, 1658 (2000).
 - [10] C. Backx, G. R. Wight, and M. J. Van der Wiel, J. Phys. B **9**, 315 (1976).
 - [11] W. Wolff *et al.*, Phys. Rev. A **65**, 042710 (2002).
 - [12] M. A. Abdallah *et al.*, Phys. Rev. A **62**, 012711 (2000).
 - [13] M. E. Galassi *et al.*, Phys. Rev. A **66**, 052705 (2002).
 - [14] W. A. Chupka and J. Berkowitz, J. Chem. Phys. **51**, 4244 (1969).
 - [15] P. M. Dehmer and W. A. Chupka, J. Chem. Phys. **65**, 2243; **66**, 1972 (1976).
 - [16] R. S. Berry and S. E. Nielsen, Phys. Rev. A **1**, 383; **1** 395 (1970).
 - [17] G. Herzberg and Ch. Jungen, J. Mol. Spectrosc. **41**, 425 (1972).
 - [18] V. H. Dibeler, R. M. Reese, and M. Krauss, J. Chem. Phys. **42**, 2045 (1965).
 - [19] M. Inokuti, Rev. Mod. Phys. **43**, 297 (1971).
 - [20] R. M. Wood, A. K. Edwards, and M. F. Steuer, Phys. Rev. A **15**, 1433 (1977).
 - [21] Y. M. Chung *et al.*, J. Chem. Phys. **99**, 885 (1993).
 - [22] Z. X. He *et al.*, J. Chem. Phys. **103**, 3912 (1995).
 - [23] I. Sánchez and F. Martín, J. Chem. Phys. **107**, 8391 (1997).
 - [24] T. E. Sharp, At. Data Nucl. Data Tables **2**, 119 (1971).
 - [25] S. L. Guberman, J. Chem. Phys. **78**, 1404 (1983).